PHYSICAL REVIEW B VOLUME 26, NUMBER 6 15 SEPTEMBER 1982

Theory of lattice-dynamical properties of solids: Application to Si and Ge

M. T. Yin* and Marvin L. Cohen
Department of Physics, University of California, and Materials and Molecular Research Division, Lawrence Berkeley Laboratory, Berkeley, California 94720

(Received 1 March 1982)

It is demonstrated that the *ab initio* pseudopotential theory within the local-density-functional formalism provides an accurate theoretical framework for the study of lattice-dynamical properties of solids. With the use of atomic numbers and masses of constituent elements and the crystal structure as the only input information, the calculated phonon frequencies and mode-Grüneisen parameters at Γ and X, the third-order force constant for LTO (Γ), the shear modulus, and the zone-center TA [110] velocity are all in excellent agreement with experiment. Comparison with other microscopic calculations is made.

I. INTRODUCTION

In this paper, we present an *ab initio* microscopic theory for the lattice-dynamical properties of solids and demonstrate that the theory yields a variety of properties such as selected phonon frequencies of Si and Ge in excellent agreement with experiment. Part of the results have been briefly reported previously.[1] The theory is based on an *ab initio* pseudopotential method within the local-density-functional formalism.[2] The lattice dynamical properties are studied with the use of the frozen-phonon approach.[3-5]

The lattice dynamics of tetrahedrally coordinated semiconductors has been an active area of research in solid-state physics.[6] One of the most interesting features of the phonon spectra of these materials is that the TA modes are low lying in energy with dispersion curves which become flat away from the zone center. An early phenomenological analysis[7] of the dispersion curves using the force constant model indicates that the interatomic interaction extends to fifth-nearest neighbors. Subsequently, a variety of phenomenological models have been used to fit the phonon dispersion of semiconductors,[8] among which a six-parameter valence force-field model[9] and a four-parameter adiabatic bond-charge model[10] yield phonon dispersion curves for covalent semiconductors in rather good agreement with experiment.

There are two commonly used approaches in the microscopic studies of lattice dynamics of covalent semiconductors: the dielectric function approach[11] and the frozen-phonon approach.[3-5] Both approaches have been applied[5,12-15] to covalent semiconductors, in particular Si using pseudopotentials fitted to experimental excitation data such as the atomic (or ionic) excitation energies or bulk excitation spectra. These studies have helped to advance the microscopic understanding of lattice vibrations and fair agreement with measured phonon dispersion curves was achieved. However, various additional assumptions have been utilized in these studies, such as the introduction of a multiplicative constant to satisfy the acoustic sum rule,[12] the Hartree approximation for the inversion of dielectric matrices,[12-15] the truncation of a continued-fraction series, and the use of a constant parameter E_0 for a k-dependent function,[14] and an *ad hoc* linear repulsive force between nearest neighbors.[5,16] The use of empirically fitted pseudopotentials and additional assumptions make it difficult to ascertain whether the lattice dynamical properties can be accurately calculated using only the essential input of atomic identities and crystal structures.

The present study represents the first *ab initio* lattice dynamical calculation in which the only input information consists of the atomic numbers, atomic masses of the constituent elements, and the crystal structure; no *ad hoc* assumptions are made. The excellent agreement of the results with experiment demonstrates that the local-density-functional formalism yields accurate results for lattice dynamics. Recently, an all-electron calculation[17] on the phonon properties at Γ and X of Si has basically confirmed our findings[1] and gives, in addition, the internal strain parameter and the cubic force constant for TO (Γ) in excellent agreement with experiment.

In the following section, we will first discuss the momentum-space formulation[18] for the calculations of total energies and atomic forces and present a careful treatment of the divergent problem caused by the long-range Coulomb interaction. A generalized frozen-phonon approach is then presented. In Sec. III the calculation procedures are discussed in detail. The results of calculation for Si and Ge are given in Sec. IV. In Sec. V our results are discussed and compared with other work. Final conclusions are given in Sec. VI. In the Appendix, we show that the convergence of the phonon frequencies at Γ with respect to the dimension of the dielectric matrix is rather slow.

II. THEORY

A. Total energies and atomic forces

Almost all of the lattice dynamical properties of solids can be derived from a knowledge of the total energy[19] (E_{tot}) of solids as a function of atomic positions. To calculate E_{tot} from first principles, we employ three approximations: (i) the adiabatic (Born-Oppenheimer) approximation[20] in which the electrons are assumed to be in the ground state with respect to the instantaneous nuclear positions and the ground-state energy (i.e., E_{tot}) is then the effective potential for the nuclear motions, (ii) the local-density-functional approximation[2] in which the electronic exchange-correlation interaction is approximated by a local density functional, and (iii) the pseudopotential approximation[21] in which the interactions between valence electrons and atomic cores are simulated by pseudopotentials.

In the crystalline total energy calculation, it is advantageous to transform the real space integrals into summations in momentum space. The momentum-space formalism has been derived by Ihm, Zunger, and Cohen.[18] In the following, we will discuss the momentum-space formalism for the total energies of crystalline solids and solve the problem of the divergences in the zero-momentum components using simple arguments instead of employing a limit procedure for small $\vec{G}$.

The total energy of the crystal in the pseudopotential theory can be expressed as follows (rydberg units are used):

$$E_{\text{tot}}=E_{\text{kin}}+E_{\text{ec}}+E_H+E_{\text{xc}}[\rho]+E_{\text{cc}}\ , \tag{1}$$

where

$$E_{\text{kin}}=\sum_i n_i\int d\vec{r}\,\psi_i^*(\vec{r})(-\nabla^2)\psi_i(\vec{r})\ , \tag{2}$$

$$E_{\text{ec}}=\sum_{i,\vec{l},s} n_i\int d\vec{r}\,\psi_i^*(\vec{r})\hat{v}_s(\vec{r}-\vec{l}-\vec{\tau}_s)\psi_i(\vec{r})\ , \tag{3}$$

$$E_H=\tfrac{1}{2}\int dr\,\rho(\vec{r})V_H(\vec{r}), \tag{4}$$

$$E_{\text{cc}}=\frac{N}{2}\sum_{\vec{l},s,s'}{}'\frac{2Z_sZ_{s'}}{|\vec{l}+\vec{\tau}_s-\vec{\tau}_{s'}|}\ , \tag{5}$$

$$\rho(\vec{r})=\sum_i n_i\,|\,\psi_i(\vec{r})\,|^2\ . \tag{6}$$

The symbols n_i and $\psi_i(\vec{r})$ are, respectively, the occupation number and the (pseudo) wave function for the one-electron state i. N is the number of cells in the crystal, and $\vec{l}$ is the lattice vector. The symbols Z_s and $\vec{\tau}_s$ are, respectively, the core charge and the basis vector for atom s in the cell, and $\hat{v}_s$ is its core pseudopotential. In general, $\hat{v}_s$ is angular-momentum dependent (nonlocal) and can be expressed as

$$\hat{v}_s(\vec{r})=\sum_l v_{s,l}(r)\hat{\mathscr{P}}_l\ , \tag{7}$$

where $\hat{\mathscr{P}}_l$ is the projection operator for angular momentum l. The carets are used to denote nonlocal operators, and the summation over l goes from zero to infinity.

The expression for E_{kin} has the form of the electronic kinetic energy and may be interpreted as such. A word of caution is in order. When the atom is pseudized, the kinetic energy and the potential energy are mixed in a complicated way. Hence, E_{kin} in the pseudopotential case has no direct relationship with the all-electron counterpart. The remaining contributions are as follows: E_{ec} is the electron-core interaction energy, E_H is the electron-electron Coulomb energy (Hartree energy), and E_{cc} is the core-core Coulomb energy. Here we assume that atomic cores are well localized and the overlapping between them usually described by a Born-Mayer potential and van der Waals interaction is negligible. This assumption breaks down if atoms are brought so closely together that atomic cores overlap with each other appreciably. The prime in the summation of Eq. (5) excludes the term in which $\vec{l}=\vec{l}\,'$ and $s=s'$. $E_{\text{xc}}[\rho]$ is the electronic exchange-correlation energy. Within the local-density-functional approximation, it can be expressed by:

$$E_{\text{xc}}[\rho]\cong\int\rho(\vec{r})\epsilon_{\text{xc}}(\rho(\vec{r}))d\vec{r}\ , \tag{8}$$

where $\epsilon_{\text{xc}}(\rho(\vec{r}))$ is a function of $\rho(\vec{r})$ and may be interpolated from exchange-correlation energies calculated for the systems of an interacting homogeneous electron gas with various densities. The $\vec{r}$-space integrations are over the whole crystal volume Ω, and the energies are also for the whole crystal. The electrons mentioned here and henceforth refer to the valence electrons only.

Because of the long-range nature of the Coulomb interaction, E_{ec}, E_H, and E_{cc} diverge individually. They all have an infinite zero-momentum term when expressed by summations in momentum space. Let us first decompose E_{ec} into a divergent Coulomb interaction energy between valence electrons and cores,

$$E_{\text{ec}}^{\text{Coul}}=\int d\vec{r}\rho(\vec{r})\left[\sum_{\vec{l},s}\frac{-2Z_s}{|\vec{r}-\vec{R}_{\vec{l},s}|}\right] \tag{9}$$

and a remaining finite part. Then, the sum E_{Coul} of $E_{\text{ec}}^{\text{Coul}}$, E_H, and E_{cc} is just the electrostatic energy of the system consisting of a periodic distribution $\rho(\vec{r})$ of electrons in a lattice of positive point charges. We may now add a positive and a negative background to the system and divide the whole system into a subsystem A composed of a lattice of positive point charges plus a neutralizing negative background and a subsystem B composed of a periodic electronic distribution $\rho(\vec{r})$ plus a neutralizing positive background. Because of the superposition property of the Coulomb interaction, E_{Coul} is the sum of the Coulomb energy E^A of subsystem A, the Coulomb energy E^B of subsystem B, and the Coulomb interaction energy E^{AB} between subsystems A and B. E^A is just the Ewald energy which we will denote as E'_{cc} henceforth. E^B and E^{AB} can then be expressed in momentum space as summations over the reciprocal-lattice vector $\vec{G}$:

$$E^B=\frac{\Omega}{8\pi}\sum_{\vec{G}}|\vec{E}_B(\vec{G})|^2\,, \tag{10}$$

$$E^{AB}=\frac{\Omega}{4\pi}\sum_{\vec{G}}\vec{E}_A^*(\vec{G})\cdot\vec{E}_B(\vec{G})\,, \tag{11}$$

where $\vec{E}_A$ and $\vec{E}_B$ are the Fourier transforms of the electric fields of subsystem A and subsystem B, respectively. Now that the cell average (i.e., the zero-momentum term) of the electric field vanishes in a periodic system, the $\vec{G}=0$ terms in Eqs. (10) and (11) are identically zero, and thus can be excluded from the summations. We may then use Poisson's equation and obtain alternative expressions for Eqs. (10) and (11):

$$E^B=\frac{\Omega}{2}\sum_{\vec{G}}{}'\frac{8\pi}{|\vec{G}|^2}|\rho(\vec{G})|^2\,, \tag{12}$$

$$E^{AB}=\Omega\sum_{\vec{G}}{}'\rho^*(\vec{G})V^A(\vec{G})\,, \tag{13}$$

where $V^A(\vec{G})$ is the Fourier transform of

$$\sum_{\vec{l},s}\frac{-2Z_s}{|\vec{r}-\vec{R}_{\vec{l},s}|}\,.$$

The prime signs in Eqs. (12) and (13) indicate that the zero-momentum terms are excluded from the summations. We note that in a physical system $\rho(\vec{G})$ decreases rapidly as $|\vec{G}|$ increases so that the summations in Eqs. (12) and (13) are convergent.

In practical calculations, it is advantageous to further decompose the *ab initio* core pseudopotential into

$$\hat{v}_s(r)=v_s(r)+\sum_{l=0}^{\infty}v'_{s,l}(r)\hat{\mathscr{P}}_l\,, \tag{14}$$

where

$$v'_{s,l}(r)=v_{s,l}(r)-v_s(r) \tag{15}$$

and the local potential $v_s(r)$ has the $-2Z_v/r$ Coulomb tail but does not have the $1/r$ singularity at the origin. This term can be chosen from the $v_{s,l}$'s. The potential $v'_{s,l}(r)$ is then a short-range function of r. After Fourier transformation, we then obtain the expression of the total energy *per cell:*

$$E_{\text{tot}}=E_{\text{kin}}+E'_{\text{ec}}+E'_H+E_{\text{xc}}+E'_{\text{cc}} \tag{16}$$

with individual energy contributions expressed as follows:

$$E_{\text{kin}}=\frac{1}{N}\sum_{i,\vec{G}}n_i\,|\psi_i(\vec{k}_i+\vec{G})|^2(\vec{k}_i+\vec{G})^2\,, \tag{17}$$

$$E'_{\text{ec}}=\Omega_c\sum_{s,\vec{G}}\rho^*(\vec{G})e^{-i\vec{G}\cdot\vec{\tau}_s}v_s(\vec{G})+\sum_{i,\vec{G},\vec{G}',s,l}[n_i\psi_i^*(\vec{k}_i+\vec{G})\psi_i(\vec{k}_i+\vec{G}')e^{i(\vec{G}-\vec{G}')\cdot\vec{\tau}_s}v'_{s,l}(\vec{k}_i+\vec{G},\vec{k}_i+\vec{G}')]\,, \tag{18}$$

$$E'_H=\frac{\Omega_c}{2}\sum_{\vec{G}}\frac{8\pi}{|\vec{G}|^2}|\rho(\vec{G})|^2 , \tag{19}$$

$$E_{\mathrm{xc}}=\Omega_c\sum_{\vec{G}}\rho^*(\vec{G})\epsilon_{\mathrm{xc}}(\vec{G}) , \tag{20}$$

$$E'_{\mathrm{cc}}=\tfrac{1}{2}\sum_{s,s'}2Z_sZ_{s'}\left[\frac{4\pi}{\Omega_c}\sum_{\vec{G}}{}'\frac{1}{|\vec{G}|^2}\cos[\vec{G}\cdot(\vec{\tau}_s-\vec{\tau}_{s'})]\exp\left[-\frac{|\vec{G}|^2}{4\eta^2}\right]-\frac{\pi}{\eta^2\Omega_c}+\sum_{\vec{l}}{}'\left[\frac{\mathrm{erfc}(\eta x)}{x}\right]_{x=|\vec{l}+\vec{\tau}_s-\vec{\tau}_{s'}|}-\frac{2\eta}{\sqrt{\pi}}\delta_{ss'}\right] , \tag{21}$$

Ω_c is the cell volume ($\Omega_c=\Omega/N$). The primes in the $\vec{G}$ summations exclude the $\vec{G}=0$ term. The prime in the $\vec{l}$ summation in Eq. (21) excludes the $\vec{l}=0$ term when $s=s'$; η is a parameter controlling the convergency of the Ewald summations.[22] The symbols k_i and ψ_i are, respectively, the crystal momentum and the wave function in momentum space of state i.

For nonzero $\vec{G}$'s, $v_s(\vec{G})$ in Eq. (18) is the Fourier transform of $v_s(r)$, i.e.,

$$v_s(\vec{G}\neq 0)\equiv\frac{1}{\Omega_c}\int d\vec{r}\,e^{-i\vec{G}\cdot\vec{r}}v_s(r) . \tag{22}$$

The zero-momentum term of $v_s(\vec{G})$ is defined as follows:

$$v_s(G=0)\equiv\frac{1}{\Omega_c}\int d\vec{r}\left[v_s(r)+\frac{2Z_s}{r}\right] , \tag{23}$$

which is part of the zero-momentum term of the Fourier transform of $v_s(r)$. The other part is the zero-momentum term of the Coulomb interaction ($-2Z_s/r$), which has been shown above to cancel with the divergent terms in E_H and E_{cc}. The primes in Eq. (16) indicate the exclusion of the canceling infinite zero-momentum contributions. The Fourier transform of $v'_{s,l}(r)\hat{\mathcal{P}}_l$ in Eq. (18) has the functional form:

$$v'_{s,l}(\vec{k},\vec{k}')=\frac{4\pi}{\Omega_c}(2l+1)P_l\left[\frac{\vec{k}\cdot\vec{k}'}{|\vec{k}|\,|\vec{k}'|}\right]\int_0^\infty v'_{s,l}(r)j_l(|\vec{k}|r)j_l(|\vec{k}'|r)r^2dr , \tag{24}$$

where P_l and j_l are, respectively, Legendre and spherical Bessel functions.

The momentum-space formalism is closely related to the plane-wave method for the calculation of electronic structures. The Schrödinger equation used in the plane-wave method can be easily derived variationally from the expression for the total energy in Eq. (16). Using the resulting eigenvalues ϵ_i's, we obtain an alternative expression for the total energy (per cell):

$$E_{\mathrm{tot}}=\frac{1}{N}\sum_i n_i\epsilon_i-E'_H+\Delta E_{\mathrm{xc}}+E'_{\mathrm{cc}} , \tag{25}$$

where

$$\Delta E_{\mathrm{xc}}=\Omega_c\sum_{\vec{G}}\rho^*(\vec{G})[\epsilon_{\mathrm{xc}}(\vec{G})-V_{\mathrm{xc}}(\vec{G})] \tag{26}$$

and V_{xc} is the exchange-correlation potential,

$$v_{\mathrm{xc}}=\frac{d(\rho\epsilon_{\mathrm{xc}})}{d\rho} . \tag{27}$$

The double summation over $\vec{G}$'s in Eq. (18) is absorbed in the simple summation of the eigenvalues of the occupied states in Eq. (25).

The force $\vec{F}^s$ acting on atom s is the negative derivative of E_{tot} (per cell) with respect to a basis vector $\vec{\tau}_s$. The terms containing implicit derivatives of the wave functions vanish (Hellmann-Feynman theorem)[23,18] and a simple expression is derived as follows:

$$\vec{F}^s=\vec{F}_e^s+\vec{F}_c^s\ , \tag{28}$$

where

$$\vec{F}_e^s=-\left.\frac{\partial E'_{\rm ec}}{\partial\vec{\tau}_s}\right|_{\psi}=i\Omega_c\sum_{\vec{G}}\rho^*(\vec{G})\vec{G}e^{-i\vec{G}\cdot\vec{\tau}_s}v_s(\vec{G})-i\sum_{i,\vec{G},\vec{G}',l}[n_i\psi_i^*(\vec{k}_i+\vec{G})\psi_i(\vec{k}_i+\vec{G})(\vec{G}-\vec{G}')$$

$$\times e^{i(\vec{G}-\vec{G}')\cdot\vec{\tau}_s}v'_{s,l}(\vec{k}_i+\vec{G},\vec{k}_i+\vec{G}')]\ , \tag{29}$$

$$\vec{F}_c^s=-\frac{dE'_{\rm cc}}{d\vec{\tau}_s}=2Z_s\sum_{s'\neq s}Z_{s'}\left[\frac{4\pi}{\Omega_c}\sum_{\vec{G}}{}'\left(\frac{\vec{G}}{|\vec{G}|^2}\sin[\vec{G}\cdot(\vec{T}_s-\vec{\tau}_{s'})]\exp(-|G|^2/4\eta^2)\right)\right.$$

$$\left.+\sum_{\vec{l}}\left(\frac{\vec{x}\,\mathrm{erfc}(\eta|\vec{x}|)}{|\vec{x}|^3}+\frac{2\eta\vec{x}}{\sqrt{\pi}|\vec{x}|^2}e^{-|\vec{x}|^2}\right)_{\vec{x}=\vec{l}+\vec{\tau}_s-\vec{\tau}_{s'}}\right]\ , \tag{30}$$

$\vec{F}_e^s$ is the force contribution from the valence electrons, and $\vec{F}_c^s$ is the force contribution from the other atomic cores.

B. Lattice-dynamical study

In principle, any phonon with lattice momentum commensurate with the reciprocal lattice vectors can be studied using the method presented in the preceding section for periodic lattices. For such phonons, there exists a superlattice in which the motions of corresponding atoms in different supercells are identical. We can perform microscopic calculations of the total energy and atomic forces as a function of the atomic positions in the supercell. The dynamical matrix for the atoms in the supercell can then be constructed in the harmonic approximation and the phonon frequencies and polarizations obtained. The microscopic calculations also provide information about anharmonic contributions. In fact, such calculations are capable of yielding all lattice-dynamical information for phonons of lattice momenta commensurate with the reciprocal-lattice vectors.

In practice, the supercell calculation is limited by the computational capability in both speed and memory. The maximum feasible number of atoms in a supercell is of the order of 10. When the number of atoms in a supercell is large, another problem arises. Since the number of degrees of freedom (N_f) becomes large, one has to calculate total energies for a large number ($\propto N_f^2$) of distorted geometries to determine the dynamical matrix. The calculations of (Hellmann-Feynman) atomic forces are very useful in this respect. The number of distorted geometries required is relatively small ($\propto N_f$). A knowledge of the symmetry properties also greatly simplifies the determination of the form of the dynamical matrix and of eigenvectors for phonons with lattice momentum at a symmetry point in the Brillouin zone.

III. CALCULATIONS

Using the atomic numbers as input, the *ab initio* pseudopotentials of Si and Ge are generated using the Hamann-Schlüter-Chiang scheme.[24] These *ab initio* pseudopotentials have been shown[1,25] to give accurate static structural properties and phase transformation properties. In particular, the equilibrium lattice constants of Si and Ge are in excellent agreement with experiment to within 1%. This serves as a prerequisite for the present study of lattice dynamical properties of Si and Ge. A discussion of *ab initio* pseudopotentials will be given elsewhere.[21]

In this paper, we study the phonon properties at Γ and X for Si and Ge. By symmetry, the LO and TO modes at Γ are degenerate [referred to as LTO(Γ)], and so are the LO and LA modes at X [referred to as LOA(X)]. Since the phonon polarizations at these points of the diamond lattice are readily determined by group-theoretic method

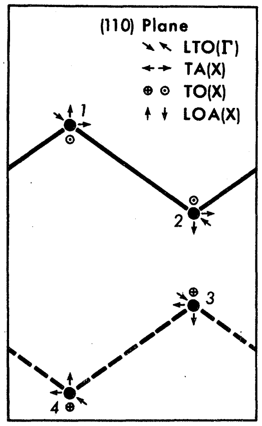

FIG. 1. Phonon polarization at Γ and X $(0,0,2\pi/a)$ for the diamond structure. Atoms are numbered and denoted by black dots. The solid lines denote an atomic chain in a (110) plane, and the dashed lines denote the projection of an atomic chain a distance $\sqrt{2}a/4$ away from that plane where a is the lattice constant.

(shown in Fig. 1), the 6×6 dynamical matrices can be decomposed to 1×1 matrices if the phonon polarization vectors are chosen as normal coordinates.

The primitive cell for the phonon-distorted lattice contains two atoms for LTO (Γ) and four atoms for phonons at X. The point group for the phonon-distorted lattice is D_{3d} (symmorphic) for LTO (Γ) and D_{2h} (nonsymmorphic) for phonons at X with different nonsymmorphic translation vectors for different modes. All these phonon-distorted lattices have inversion symmetry, which facilitates the computation.

The force constant for a normal mode at Γ or X of the diamond lattice can be obtained from the second derivative of $E_{\text{tot}}(u)$ (per atom) with respect to the amplitude u of the phonon distortion,

$$k=\left.\frac{\partial^2 E_{\text{tot}}}{\partial u^2}\right|_{u=0}\cong\frac{2\Delta E_{\text{tot}}(u)}{u^2} \tag{31}$$

or from the atomic force $F(u)$,

$$k=-\left.\frac{\partial F}{\partial u}\right|_{u=0}\cong-\frac{F(u)}{u}\,, \tag{32}$$

where

$$\Delta E_{\text{tot}}(u)=E_{\text{tot}}(u)-E_{\text{tot}}(0)\ . \tag{33}$$

The phonon frequency is then,

$$f=\sqrt{k/M}\,/2\pi\,, \tag{34}$$

where M is the atomic mass.

In the following, we will discuss the procedures for the calculations of the total energies and atomic forces. For each phonon-distorted lattice, we solve the one-electron Schrödinger equation iteratively to self-consistency,[26] at which point the maximum difference between the input and the output screening potential in momentum space is less than 10^{-5} Ry and the total energy and the atomic forces are stable to within 10^{-6} Ry and 10^{-4} Ry$/a_B$, respectively (a_B is the Bohr radius). The Wigner interpolation formula[27] for the exchange-correlation energy is used. The number of plane waves used in the basis set is increased until the phonon frequencies converged to about 0.2 THz. For phonon modes at X, about 300 plane waves are used for Si and 400 plane waves are used for Ge, which corresponds to a plane-wave kinetic energy cutoff of 10 Ry for Si and 12 Ry for Ge. For LTO (Γ), the number of plane waves used is smaller by a factor of 2 because of a smaller number of basis atoms. The set of special k points[28] used is $\{(\frac{1}{4},\frac{1}{4},\frac{1}{4}),(-\frac{1}{4},\frac{1}{4},\frac{1}{4}),(\frac{3}{4},\frac{1}{4},\frac{1}{4}),(-\frac{3}{4},\frac{1}{4},\frac{1}{4}),(\frac{3}{4},-\frac{1}{4},\frac{1}{4})\}$ (Cartesian coordinates in units of $2\pi/a$ where a is the lattice constant) in the irreducible $\frac{1}{12}$ Brillouin zone for LTO (Γ) and $\{(\frac{1}{8},\frac{1}{8},\frac{1}{4}),(\frac{1}{8},\frac{3}{8},\frac{1}{4}),(\frac{3}{8},\frac{1}{8},\frac{1}{4}),(\frac{3}{8},\frac{3}{8},\frac{1}{4})\}$ (in the reciprocal lattice coordinates) in the irreducible $\frac{1}{8}$ Brillouin zone for phonons at X. The convergent error of the phonon frequencies with respect to the number of sampling k points is about 0.2 THz.

IV. RESULTS

For each phonon mode at Γ or X, we calculate total energies and atomic forces of the phonon-distorted lattices with five different amplitudes ranging from 0.01 to 0.1 Å. The total energies can be well represented (to about 1%) by a quadratic function of the amplitude except for the LTO (Γ) mode for which a third-order term is needed for a good fit. The phonon frequencies can then be deduced and are compared to experiment in Table I. The agreement with experiment[29,30] is excellent. We note, in particular, that the low-lying TA(X) mode is well described.

For LTO (Γ), there is a third-order anharmonic term and a cubic force constant k_{xyz} may be defined as follows:

$$\Delta E_{\text{tot}}(u)=\frac{k}{2}u^2+4k_{xyz}\left[\frac{u}{\sqrt{3}}\right]^3\ . \tag{35}$$

The experimental value of k_{xyz} can be deduced from the measured third-order elastic force constants[31]: In the deduction, the third-order elastic

TABLE I. Comparison of calculated phonon frequencies (in THz) of Si and Ge at Γ and X with experiment (Refs. 29 and 30) ($f_{\rm expt}$). The values for f_E (f_F) are obtained from energy (force) calculations. The deviations from experimental values are given in parentheses.

	LTO (Γ)	LOA (X)	TO (X)	TA (X)
Si				
f_E	15.16(−2%)	12.16(−1%)	13.48(−3%)	4.45(−1%)
f_F	15.14(−3%)	11.98(−3%)	13.51(−3%)	4.37(−3%)
$f_{\rm expt}$	15.53	12.32	13.90	4.49
Ge				
f_E	8.90(−2%)	7.01(−3%)	7.75(−6%)	2.44(2%)
f_F	8.89(−3%)	6.96(−3%)	7.78(−6%)	2.45(2%)
$f_{\rm expt}$	9.12	7.21	8.26	2.40

force constants are fitted to the theoretical expressions in Keating's model[32] involving three anharmonic force constants. Within Keating's model, k_{xyz} equals to 16γ where γ is one of the anharmonic force constants defined in Ref. 32. The calculated values of k_{xyz} for Si and Ge are compared to the deduced values in Table II. The agreement is excellent. We note that the values of k_{xyz} are negative, which means that it is more difficult to compress a bond than to stretch it.

The phonon frequencies and k_{xyz} can also be obtained from the calculated atomic forces.[33] The results are also given in Tables I and II. It is found that the results obtained from the force calculation are very close to those obtained from the energy calculation. This demonstrates that force calculations using the self-consistent pseudopotential method can be done very accurately. Some detailed information can also be obtained from the force calculation. For the LOA (X) mode, the forces on atom 2 and on atom 3 (Fig. 1) are not the same for a finite amplitude. For an amplitude of 0.108 Å the corresponding force constants are 15.86 eV/Å^2 for atom 2 and 17.37 eV/Å^2 for atom 3. The force constant difference varies linearly with respect to amplitude. This represents another case of anharmonicity. The two different force constants also indicate that it is harder to compress a bond than to stretch it. The average of these two force constants, however, does not vary with the amplitude to within 0.5% and it is used for the phonon calculation.

TABLE II. Comparison of the cubic force constant k_{xyz} (in eV/ Å^3) of Si and Ge with experiment (Refs. 31 and 32). The values for k_{xyz}^E (k_{xyz}^F) are obtained from energy (force) calculations.

	Si	Ge
k_{xyz}^E	−32.8	−27.7
k_{xyz}^F	−32.6	−28.1
$f_{xyz}^{\rm expt}$	−35.1	−27.2

As described in the preceding section, the convergency of the calculated results with respect to the number of sampling k points and the kinetic energy cutoff $E_{\rm pw}$ of the plane-wave expansion has been carefully examined. In Table III, we give results for phonon frequencies of Si and Ge calculated with different $E_{\rm pw}$'s. Except for the TA (X) mode, the phonon frequencies are convergent to less than 10% for small $E_{\rm pw}$'s (4−6 Ry). This convergent test provides useful information about error estimates for other studies with the use of the *ab initio* pseudopotential approach, e.g., the structural study of the Si(001)-(2×1) surface,[34] in which, $E_{\rm pw}$ is relatively limited by the computational capability and memory size of the computer.

The most important features of the TA modes of Si and Ge, as well as other cubic tetrahedrally coordinated semiconductors, are that the TA dispersion curves are low-lying in energy and become flat away from the zone center. The low-lying feature has already been demonstrated above with the TA (X) mode. The flatness feature can be demonstrated by calculating directly the entire dispersion relation along a specific direction, like the [001] direction using an *ab initio* interlayer force constant approach. This has been done by the authors and is presented elsewhere.[35] Here we will demonstrate that the TA velocity, i.e., the rising slope of the dispersion curve, at the zone center is rather large. This is an important ingredient related to the flatness of the TA modes.

The zone-center TA velocity v chosen is the one propagating along the [110] direction with [1$\bar{1}$0] polarization. This velocity is associated with the shear modulus $C_{11}-C_{12}$ by

TABLE III. Convergency test of the phonon frequencies of Si and Ge (from energy calculations) with respect to the cutoff energy E_{pw} for a plane-wave expansion. Frequencies are in units of THz.

E_{pw} (Ry)	LTO (Γ)	LOA (X)	TO (X)	TA (X)
Si				
4.5	15.55	12.85	14.28	5.45
6	14.33	11.73	12.75	5.02
7.6	14.69	11.86	12.94	4.69
9	15.06	12.06	13.32	4.54
10	15.16	12.16	13.48	4.45
Ge				
6	8.64	7.10	7.69	3.31
8	8.71	7.05	7.54	2.84
10	8.77	6.94	7.58	2.54
12	8.90	7.01	7.75	2.44

$$v=\left[\frac{(C_{11}-C_{12})}{2\rho_M}\right]^{1/2}, \tag{36}$$

where ρ_M is the mass density.

We introduce a homogeneous tetragonal distortion into the diamond lattice, in which the length scales of the three cubic directions are changed by $1+\epsilon$, $1+\epsilon$, and $(1+\epsilon)^{-2}$, respectively, while the atomic volume Ω_a are kept constant. The change ΔE_{tot} (per atom) is related to $C_{11}-C_{12}$ by

$$\Delta E_{\mathrm{tot}}=3\Omega_a(C_{11}-C_{12})\epsilon^2+O(\epsilon^3)\ . \tag{37}$$

The third-order contribution can be eliminated by averaging $\Delta E_{\mathrm{struc}}(\epsilon)$ and $\Delta E_{\mathrm{struc}}(-\epsilon)$. Total energies are calculated with the value of ϵ varying from 0 to $\pm$ 0.04. The shear modulus $C_{11}-C_{12}$ and the associated TA velocity are obtained from Eqs. (37) and (36). These values for both Si and Ge are in excellent agreement with experiment[36] as shown in Table IV.

It is interesting to examine the individual contributions to the force constants for the phonon modes at Γ and X and to the quantity $2a(C_{11}-C_{12})$ for Si and Ge. These are given in Table V. The individual contributions are defined in Eqs. (16), (31), and (37). The finite amplitude used is $\pm 0.01a$ for LTO (Γ), $0.02a$ for LOA (X), and $0.0177a$ for TO (X) and TA (X) where a is the lattice constant. We note that the sign of each contribution is the same for LTO (Γ), LOA (X) and TO (X), whereas TA (X) and $2a(C_{11}-C_{12})$ have opposite signs. This can be explained as follows: The TA (X) mode and the $C_{11}-C_{12}$ shear mode involve bond bending in first order, bond stretching in second order, and no bond compression. As a result, the valence charge density of the distorted lattices become more evenly distributed than that of the ideal lattice, which leads to decreases in E_{kin} and E'_H and increases in E'_{ec} and E_{xc}. (The change in E'_{cc} can also be qualitatively explained by bond-length changes.) In contrast, the opposite is true for other modes where bond lengths are changed in first order and the valence charge density becomes less uniformly distributed.

TABLE IV. Comparison of calculated values of $C_{11}-C_{12}$ and the TA velocity along [110] (with [1$\bar{1}$0] polarization) of Si and Ge with experiment (Ref. 36).

	$C_{11}-C_{12}$ (Mbar)	$v_{\mathrm{TA}\,[110]}$ (10^5 cm/sec)
Si		
Theory	1.07	4.79
Expt.	1.027	4.693
Ge		
Theory	0.74	2.64
Expt.	0.819	2.770

For the LTO (Γ), LOA (X), and TO (X) modes, the Ewald contribution plays a dominant role in stabilizing the system and the electronic contribution reduces the Ewald contribution in the form of screening.[5] In contrast, the Ewald contribution (k'_{cc}) for TA (X) as well as for $2a(C_{11}-C_{12})$ is negative, which means that the lattice is unstable with respect to shear distortions associated with the TA (X) mode and $C_{11}-C_{12}$ if the electrons are nonresponsive. The electronic contribution (k_e), i.e., the sum of k_{kin}, k'_{ec}, k'_H, and k_{xc}, overcompensates the Ewald effect and stabilizes the diamond structure. This is a manifestation of the directional covalent bonds. Since the total contributions for

TABLE V. Contributions to force constants for phonon modes at and X of (a) Si and (b) Ge and contributions to the quantity $2a(C_{11}-C_{12})$. The theoretical results are from total energy calculations. The experimental values (Refs. 29, 30, and 36) are given in the last row. All are in units of eV/ Å^2. The electronic contribution k_e is the sum of k_{kin}, k'_{ec}, k'_H, and k_{xc}.

	LTO (Γ)	LOA (X)	TO (X)	TA (X)	$2a(C_{11}-C_{12})$
			(a) Si		
k_{kin}	30.88	11.68	32.57	−17.49	−8.58
k'_{ec}	−72.28	−109.15	−146.62	58.06	57.99
k_H	26.89	42.58	45.82	−19.39	−19.25
k_{xc}	−7.30	−0.61	−7.46	6.19	5.25
k_e	−21.82	−55.52	−75.69	27.38	35.40
k'_{cc}	48.26	72.53	96.60	−25.11	−28.14
k_{tot}	26.44	17.01	20.91	2.27	7.26
$k_{\text{tot}}^{\text{expt}}$	27.75	17.46	22.23	2.32	6.96
			(b) Ge		
k_{kin}	16.40	13.68	29.84	−10.76	−6.43
k'_{ec}	−38.27	−100.91	−131.96	45.72	49.86
k'_H	3.11	39.13	41.82	−15.64	−18.10
k_{xc}	−0.40	−1.43	−7.27	4.67	4.81
k_e	−19.15	−49.54	−67.57	23.99	30.13
k'_{cc}	42.70	64.15	85.43	−22.22	−24.90
k_{tot}	23.55	14.61	17.86	1.77	5.23
$k_{\text{tot}}^{\text{expt}}$	24.73	15.46	20.29	1.71	5.79

TA (X) and $2a(C_{11}-C_{12})$ are small, every contribution is important and should be taken into account in the calculations.

The large difference in the experimental values of k_{tot} between TA (X) and $2a(C_{11}-C_{12})$ is well described in our calculation. This gives a large rising slope at the zone center and a low-lying end point at the zone boundary for TA dispersion curves, which implies a flat TA dispersion curve away from the zone center—a prominent feature in the tetrahedrally coordinated semiconductors. It is noted that except for the kinetic energy contribution, the other contributions are almost the same between TA (X) and $2a(C_{11}-C_{12})$. It is the kinetic energy contribution that makes the total contribution of $2a(C_{11}-C_{12})$ larger than that of TA (X). This may be attributed to the fact that the Jones zone associated with the $C_{11}-C_{12}$ distortion is changing from a cubic symmetric shape[37] to an oblique shape which is more extended in one direction and less extended in the other two or vice versa. The $C_{11}-C_{12}$ distorted lattice has a larger free-electron kinetic energy averaging over the Jones zone. This gives positive contribution to E_{kin} and makes k_{kin} larger (less negative) for $2a(C_{11}-C_{12})$ than for TA (X). As a result, k_{tot} of $2a(C_{11}-C_{12})$ is larger than that of TA (X).

Figure 2(a) is a contour plot in the (110) plane of the charge-density difference between an LTO (Γ)-distorted lattice and the ideal lattice of Si. It is seen that the valence charge becomes more concentrated in the region where the bond is compressed and it becomes less concentrated when the bond is stretched. Such phenomena have been observed in Refs. 38 and 5. Figure 2(b) is a similar contour

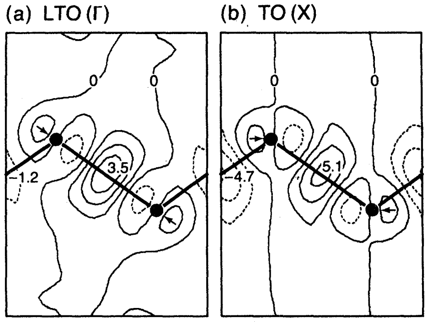

FIG. 2. (a) Contour plot of charge-density difference (in units of 0.025 e/Å ^{3}) in the (110) plane between an LTO (Γ)-distorted lattice with an amplitude of 0.054 Å and the ideal lattice of Si. The dashed contours represent negative values. The arrows indicate the atomic movements. (b) Similar plot for TO (X) with an amplitude of 0.096 Å.

plot of the charge redistribution for the TO (X) mode. The maximum charge density at the bond center varies linearly with respect to bond-length change as one may expect. It is interesting to note that the proportionality constant is, to a large extent, independent of the vibration mode. For example, the proportional constant is within -0.8 ± 0.1 $e/\text{Å}^4$ for the LTO (Γ), TO (X), and LOA (X) modes of Si. Such microscopic parameter may be useful for the phenomenological model with variable bond charges as mentioned in Ref. 8.

The charge redistribution of the TA (X) mode is different from those of other modes. As shown in Fig. 1, the atomic chains are moving against each other for the TA (X) mode. There are two ways to represent the charge redistribution. One is to take the charge density difference between the ideal lattice and the TA (X)-distorted lattice in which the atomic chain is shifted by a finite amount.[38] This representation of the charge redistribution is shown in Fig. 3(a). The prominent feature in this plot comes from a rigid shift of charge density following the motion of the atomic chain. To obtain information about charge redistribution aside from the rigid shift, we move the atomic chain in the ideal lattice by the same amount as in the TA (X) distortion such that the atomic positions are matched. The charge-density difference taken in this case has excluded the effect of a rigid shift. This is plotted in Fig. 3(b). To get a clear picture of the charge redistribution, we indicate another atomic chain in the upper left corner of Fig. 3(b). That atomic chain is not in the same (110) plane and part of its projection on the plane of Fig. 3(b) is shown with dashed lines and an open circle (atom 3). Relative to chain 1-2, atom 3 is displaced to the left, and the bond between atom 1 and atom 3 is consequently bent. This induces an increase in charge density in the upper left region of atom 1 and a decrease in the upper right region of atom 1. We also find an increase in charge density above the 1-2 bond and a decrease below, which indicates that the 1-2 bond charge (its position may be roughly assigned to the peak position in charge density) is displaced upward away from the bond center. This indicates that the bond charges tend to relax in such a way to preserve a regular tetrahedral configuration around the atoms. The charge redistributions for phonon modes of Ge are similar to those of Si, and thus, a discussion of Ge is omitted here.

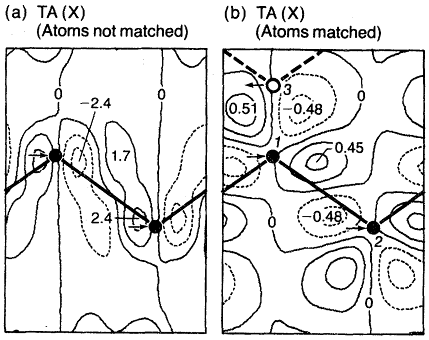
(a) TA (X) (Atoms not matched)

(b) TA (X) (Atoms matched)

FIG. 3. Contour plots of charge density difference (in units of 0.025 $e/\text{Å}^3$) in the (110) plane between a TA (X)-distorted lattice with an amplitude of 0.096 Å and ideal lattice of Si. Relative to the atomic chain (in the center of the figures) of the ideal lattice, the atomic chain of the distorted lattice is shifted to the right by an amplitude of 0.096 Å in Fig. (a). In (b), the atomic chain of the ideal lattice is rigidly shifted by the same amplitude such that the atomic chains are matched. The dashed lines denote the projection of an atomic chain a distance $\sqrt{2}a/4$ from this plane.

Another interesting feature of the TA modes is that the mode-Grüneisen parameters are negative for zone boundary phonons. We have varied the lattice constant by 1% to 3% and calculated the phonon frequencies at Γ and X for Si and Ge in a similar way. The mode-Grüneisen parameters γ can then be obtained by the following expression:

$$\gamma=-\frac{d\ln\omega}{d\ln V}\cong-\frac{\Delta\ln\omega}{\Delta\ln V}\ . \tag{38}$$

As shown in Table VI, the results are in excellent agreement with experiment including the negative value of TA (X). An analysis of various energy contributions shows that the negative value of the TA (X) mode-Grüneisen parameter comes from the fact that in that particular mode the electronic contribution plays the dominant role in stabilizing the system. When the volume becomes smaller, the system becomes more metallic and the electronic contribution which tends to increase the TA (X) frequency becomes less dominant with respect to the Ewald contribution which tends to lower the frequencies. This leads to a smaller TA (X) frequency and a negative mode-Grüneisen parameter. The experimental values of the mode-Grüneisen parameter at X of Ge are not known and our theoretical values serve as a prediction.

V. DISCUSSION

A. Pseudopotential approximation and local-density-functional approximation

Since the exact solution of the many-body Schrödinger equation of a multiatomic system is

TABLE VI. Comparison of calculated mode-Grüneisen parameters for phonons at Γ and X of Si and Ge with experiment.

	LTO (Γ)	LOA (X)	TO (X)	TA (X)
Si				
calc.	0.9	1.3	0.9	−1.5
expt.[a]	0.98	1.5	0.9	−1.4
Ge				
calc.	0.9	1.4	1.0	−1.5
expt.	1.12 ± 0.02[b] 0.88 ± 0.08[c]			

[a] Reference 39.
[b] Reference 40.
[c] Reference 41.

impossible to obtain, we employ two important approximations: the local-density-functional approximation and the pseudopotential approximation, in addition to the usual adiabatic (Born-Oppenheimer) approximation in the present study. The accuracy of these two approximations will be discussed here.

To make the pseudopotential approximation work, the effective pseudopotentials have to satisfy the "atomic requirement" that they simulate the all-electron results in the atomic limit, which includes valence eigenvalues, excitation energies, and valence wave functions outside the core region for a range of atomic configurations. Analytic justifications have been given[21] for these requirements. Numerically, these *ab initio* pseudopotentials[24,42–45] have been shown to yield band structures[24,46–48] and static structural properties of solids[49] in close agreement with the all-electron results. (We note that both the all-electron and the pseudopotential calculations within the local-density-functional formalism underestimate the measured fundamental band gap, e.g., the calculated fundamental band gap of Si is 0.5 eV compared to the experimental value of 1.17 eV). A recent all-electron study[17] has basically confirmed our present results.[1] Now we will take a different approach to illustrate the same point.

We have generated[24] a smoother *ab initio* pseudopotential[48] for Si which meets the atomic requirement, yet is not as satisfactory as the one we use. It is found that both pseudopotentials give similar static structural properties[48] and lattice dynamical properties. For example, the phonon frequencies calculated using the smooth pseudopotential are 11.93, 13.10, and 4.54 THz for LOA (X), TO (X), and TA (X) of Si, respectively. These values differ from the calculated values in Table I by about 0.2 THz and compare well with experiment. This comparison demonstrates that the calculated results are, to a large extent, independent of the parameters used in the pseudopotential generation as long as the atomic requirement is satisfied.

To examine the local-density-functional approximation, we have tested different functional forms for the exchange-correlation energy and found that the lattice dynamical results differ only by a few percent. For example, the phonon frequencies calculated using the Hedin-Lundqvist form[50] are 15.15, 12.08, 13.31, and 4.52 THz for LTO (Γ), LOA (X), TO (X), and TA (X) of Si, respectively, which differ from the results (Table I) using the Wigner form[27] by only 0.1 THz.

B. Comparison with other microscopic results

In this section, we will compare the present study with two recent microscopic studies on the phonon frequencies of Si using the frozen-phonon approach by Wendel and Martin[5] (WM) and the dielectric function approach by Van Camp, Van Doren, and Devreese[14] (VVD).

In the frozen-phonon study by WM, the pseudopotential used is fitted to the experimental excitation spectra. This empirically fitted pseudopotential does not give good static structural properties: The equilibrium lattice constant and bulk modulus are 4.7 Å and 0.70 Mbar, as compared to the experimental values of 5.43 Å and 0.99 Mbar. An *ad hoc* linear repulsive force between nearest neighbors is introduced to fit to the experimental lattice constant. We note that their calculated results depend on this *ad hoc* force parameter. In particular, the shear modulus ($C_{11} - C_{12}$) and the force constant for TA (X) change by a factor of 2 when the *ad hoc* parameter is excluded, as would be the case if a commonly used procedure[51] is taken to fit the experimental lattice constant instead of the *ad hoc* assumption. In the present study, the pseudopotential is constructed using only the atomic number as input information. Without any *ad hoc* assumptions, the calculated static structural properties and the lattice dynamical properties agree well with experiment, which demonstrates that lattice dynamical properties of solids can be accurately calculated within the local-density-functional formalism.

We have also carried out the calculation of phonon frequencies at Γ of Si using the dielectric function approach[11] and studied the dependence of the phonon frequencies with respect to the dimension of the dielectric matrix (see Appendix). It is found that if the dimension of the dielectric matrix is 27 as used in Ref. 14, the phonon frequencies at Γ are not convergent: the LA (Γ) frequency, which should be zero by symmetry, is still quite large and the LTO (Γ) frequency still has appreciable fluctuation[52] (~ 5 THz). We also find that ΔE_{xc} plays a significant role in the TA (X) mode. Its magnitude is even larger than ΔE_{tot} (see Table V). Omitting the ΔE_{xc} contribution will result in an unphysical imaginary phonon frequency. This observation implies that E_{xc} should be properly included in the dielectric matrix approach within the local-density-functional formalism.

While the results by VVD in mapping out the phonon dispersion relation of Si are remarkable, we point out that this calculation is model dependent. The reason why the LA (Γ) frequency is almost zero using a 27×27 matrix and the TA (X) frequency is positive in the Hartree approximation as obtained by VVD seems to arise from the particular model which involves the truncation of a continued-fraction series and the use of a constant parameter E_0 to replace the k-dependent μ_1/μ_0.

VI. CONCLUSION

The present study represents a unified *ab initio* calculation of the lattice dynamical properties of solids in which the only input information is the atomic numbers and masses of the constituent elements and the crystal structure. Using the atomic numbers, we generate *ab initio* pseudopotentials to simulate the interaction between valence electrons and atomic cores. With the knowledge of the crystal structure, the total energy is computed as a function of lattice constant and the calculated static structural properties including the equilibrium lattice constant are in excellent agreement with experiment when the theory is applied to crystalline Si and Ge.[1,25] This serves as a prerequisite for the lattice dynamical study. Using the frozen-phonon approach, we obtain various lattice dynamical properties of Si and Ge by total energy calculations and atomic force calculations. They include phonon frequencies at Γ and X, the third-order anharmonic force constant for LTO (Γ), the shear modulus $C_{11}-C_{12}$, the zone-center TA velocity in the [110] direction, and the mode-Grüneisen parameters for phonons at Γ and X. These results are in excellent agreement with experiment.

In particular, the frequency of the TA (X) mode is small and the zone-center TA velocity is large, which implies a flat dispersion curve as experimentally observed for both Si and Ge. An analysis of contributing factors shows that the kinetic energy has a positive contribution to make the zone-center TA velocity large and it may be attributed to a distorted Jones zone. The abnormal negative value for the mode-Grüneisen parameter of TA (X) of Si measured experimentally[39] is also well reproduced in our calculations.

The present lattice dynamical study, together with our study[1,25,48] of the static structural properties (such as the lattice constant, bulk modulus, and cohesive energy), crystal stability, and solid-solid phase transformation, represent a comprehensive structural study for two prototype semiconductors Si and Ge using a unified *ab initio* pseudopotential approach.

TABLE VII. Convergence of the phonon frequencies (in THz) of LA (Γ) and LTO (Γ) for Si with respect to the dimension of the dielectric matrix.

Dimension of the dielectric matrix	LA (Γ)	LTO (Γ)
9	5.60	21.84
15	5.60	18.29
27	3.45	17.57
51	0.97	22.84
59	0.31	20.66
65	0.84	22.67
89	0.42	20.38
113	0.41	18.38
137	0.27	18.44
Expt.[a]	0	15.53

[a] Reference 29.

ACKNOWLEDGMENTS

This work was supported by National Science Foundation Grant No. DMR7822465 and by the Director, Office of Energy Research, Office of Basic Energy Sciences, Materials Sciences Division of the U. S. Department of Energy under Contract No. DE-AC03-76SF00098.

APPENDIX

In this appendix we carry out a study of the dependence of the phonon frequencies at Γ with respect to the dimension of the dielectric matrix. The local pseudopotential given in Ref. 26 is used for the calculation of the dielectric matrix and the dynamic matrix at Γ. The Schrödinger equation is solved self-consistently using plane waves (~ 100) up to 8 Ry in kinetic energy in the basis set and another set of plane waves (~ 100) up to 12.5 Ry through Löwdin's second-order perturbation schemes.[53] An $X\alpha$ approach for E_{xc} is used and α is chosen[26] to be 0.794. Fifty conduction bands are used in the dielectric matrix calculation,[54] which includes the exchange correlation correction.[55] The subsequent dynamic matrix and phonon frequency calculations are then carried out. The resulting phonon frequencies of LA (Γ) and LTO (Γ) are given in Table VII as a function of the dimension of the dielectric matrix. [The frequency of TA (Γ) is zero.] It is found that the convergence of the phonon frequencies with respect to the dimension of the dielectric matrix is rather slow. At a dimension of 27, the LA (Γ) frequency, which should be zero because of the translational symmetry, is still very large, and the LTO (Γ) frequency still has a large fluctuation (~ 5 THz).

---

[*] Present address: Bell Laboratories, Murray Hill, New Jersey 07974.

[1] M. T. Yin and M. L. Cohen, Phys. Rev. Lett. <u>45</u>, 1004 (1980).

[2] P. Hohenberg and W. Kohn, Phys. Rev. <u>136</u>, B864 (1964); W. Kohn and L. J. Sham, *ibid.* <u>140</u>, A1133 (1965).

[3] V. Heine and D. Weaire, Solid State Phys. <u>24</u>, 249 (1970). See p. 366.

[4] D. J. Chadi and R. M. Martin, Solid State Commun. <u>19</u>, 643 (1976).

[5] H. Wendel and R. M. Martin, Phys. Rev. B <u>19</u>, 5251 (1979).

[6] For a review, see S. K. Sinha, Crit. Rev. Solid State Sci. <u>4</u>, 273 (1973).

[7] F. Herman, J. Phys. Chem. Solids <u>8</u>, 405 (1959).

[8] For a survey, see W. Weber, Phys. Rev. B <u>15</u>, 4789 (1977).

[9] A. W. Solbrig, J. Phys. Chem. Solids <u>28</u>, 2359 (1967); R. Tubino, L. Piseri, and G. Zerbi, J. Chem. Phys. <u>56</u>, 1022 (1972).

[10] W. Weber, Phys. Rev. Lett. <u>33</u>, 371 (1974), and Ref. 8.

[11] L. J. Sham, Phys. Rev. <u>188</u>, 1431 (1969); R. M. Pick, M. H. Cohen and R. M. Martin, Phys. Rev. B <u>1</u>, 910 (1970).

[12] C. M. Bertoni, V. Bortolani, C. Calandra, and E. Tosatti, Phys. Rev. Lett. <u>28</u>, 1578 (1972).

[13] S. G. Louie and M. L. Cohen, Phys. Rev. B <u>17</u>, 3174 (1978).

[14] P. E. Van Camp, V. E. Van Doren, and J. T. Devreese, Phys. Rev. Lett. <u>42</u>, 1224 (1979).

[15] R. Resta and A. Baldereschi, Phys. Rev. B <u>24</u>, 4839 (1981).

[16] See Sec. V for detailed discussions.

[17] B. N. Harmon, W. Weber, and D. R. Hamann, Phys. Rev. B <u>25</u>, 1109 (1982).

[18] J. Ihm, A. Zunger, and M. L. Cohen, J. Phys. C <u>12</u>, 4409 (1979); <u>13</u>, 3095(E) (1980).

[19] The term "total energy" used here refers to the total energy of a system of frozen nuclei. The kinetic energy of the nuclei is considered separately.

[20] M. Born and J. R. Oppenheimer, Am. J. Phys. <u>84</u>, 451 (1927).

[21] See M. T. Yin and M. L. Cohen, Phys. Rev. B <u>25</u>, 7403 (1982).

[22] See J. Ihm and M. L. Cohen, Phys. Rev. B <u>21</u>, 3754 (1980), and references therein.

[23] H. Hellmann, *Einführung in die Quanten Theorie* (Deuticke, Leipzig, 1937), p. 285; R. P. Feynman, Phys. Rev. <u>56</u>, 340 (1939); J. C. Slater, J. Chem. Phys. <u>57</u>, 2389 (1972); and Ref. 18.

[24] D. R. Hamann, M. Schlüter, and C. Chiang, Phys. Rev. Lett. <u>43</u>, 1494 (1979).

[25] M. T. Yin and M. L. Cohen, Solid State Commun. <u>38</u>, 625 (1981).

[26] M. Schlüter, J. R. Chelikowsky, S. G. Louie, and M. L. Cohen, Phys. Rev. B <u>12</u>, 4200 (1975).

[27] E. Wigner, Phys. Rev. <u>46</u>, 1002 (1934).

[28] D. J. Chadi and M. L. Cohen, Phys. Rev. B <u>8</u>, 5747 (1973); H. J. Monkhorst and J. D. Pack, *ibid.* <u>13</u>, 5189 (1976).

[29] G. Dolling, *Inelastic Scattering of Neutrons in Solids and Liquids* (IAEA, Vienna, 1963), Vol. II, p. 37 (phonon frequencies are measured at 296 K for Si); G. Nilson and G. Nelin, Phys. Rev. B <u>6</u>, 3777 (1972).

[30] G. Dolling, *Inelastic Scattering of Neutrons in Solids and Liquids* (IAEA, Vienna, 1963), Vol. II, p. 249; G. Nilsson and G. Nelin, Phys. Rev. B <u>3</u>, 364 (1971). The experimental frequencies measured at 80 K are quoted from the second reference.

[31] H. J. McSkimin and P. Andreatch, Jr., J. Appl. Phys. 35, 3312 (1965).

[32] P. N. Keating, Phys. Rev. 149, 674 (1981), and references therein.

[33] Part of the atomic-force results have been reported in J. Ihm, M. T. Yin, and M. L. Cohen, Solid State Commun. 37, 491 (1981).

[34] M. T. Yin and M. L. Cohen, Phys. Rev. B 24, 2303 (1981).

[35] M. T. Yin and M. L. Cohen, Phys. Rev. B 25, 4317 (1982).

[36] H. J. McSkimin, J. Appl. Phys. 24, 988 (1953); H. J. McSkimin and P. Andreatch, Jr., *ibid.* 34, 651 (1963); 35, 2161 (1964). The elastic moduli were measured at 77 K.

[37] V. Heine and R. O. Jones, J. Phys. C 2, 719 (1969).

[38] A. Baldereschi and K. Maschke, in *Proceedings of International Conference on Lattice Dynamics,* edited by M. Balkanski (Flammarion, Paris, 1978), Vol. 5, p. 36.

[39] B. A. Weinstein and G. J. Piermarini, Phys. Rev. B 12, 1172 (1975).

[40] C. J. Buchenauer, F. Cerdeira, and M. Cardona, in *Proceedings of the 2nd International Conference on Light Scattering in Solids,* edited by M. Balkanski (Flammarion, Paris, 1971), p. 280.

[41] K. Asaumi and S. Minomura, J. Phys. Soc. Jpn. 45, 1061 (1978).

[42] A. Redondo, W. A. Goddard III, and T. C. McGill, Phys. Rev. B 15, 5038 (1977).

[43] T. Starkloff and J. D. Joannopoulos, Phys. Rev. B 16, 5212 (1977).

[44] A. Zunger and M. L. Cohen, Phys. Rev. B 20, 4082 (1979).

[45] G. Kerker, J. Phys. C 13, L189 (1980).

[46] D. R. Hamann, Phys. Rev. Lett. 42, 662 (1979).

[47] A. Zunger, Phys. Rev. B 21, 4785 (1980).

[48] M. T. Yin and M. L. Cohen, Phys. Rev. B (in press).

[49] A. K. McMahan, M. T. Yin, and M. L. Cohen, Phys. Rev. B 24, 7210 (1981).

[50] L. Hedin and B. I. Lundqvist, J. Phys. C 4, 2064 (1971).

[51] See, e.g., N. W. Ashcroft and D. C. Langreth, Phys. Rev. 155, 682 (1967); W. Andreoni and K. Maschke, Phys. Rev. B 22, 4816 (1980).

[52] Similar results have been found in Ref. 15.

[53] P. Lowdin, J. Chem. Phys. 19, 1396 (1951).

[54] S. Adler, Phys. Rev. 126, 413 (1962); N. Wiser, *ibid.* 129, 62 (1963).

[55] S. P. Singhal and J. Callaway, Phys. Rev. B 14, 2347 (1976).

[56] We have performed total energy calculations for bulk Si with the same kinetic energy cutoff ($E_{\text{pw}}=6$ Ry). The calculated equilibrium lattice constant is 0.7% smaller than the experimental value of 5.43 Å.